East European Journal of Physics. 4. 326-335 (2023)
DOI:10.26565/2312-4334-2023-4-43 ISSN 2312-4334

NUMERICAL INVESTIGATION OF THERMOPHORESIS AND ACTIVATION ENERGY EFFECTS ON MAXWELL NANO FLUID OVER AN INCLINED MAGNETIC FIELD APPLIED TO A DISK

Dudekula Dastagiri Babu[a]*, S. Venkateswarlu[a], E. Keshava Reddy[b]
[a] *Department of Mathematics, Rajeev Gandhi Memorial College of Engineering and Technology, Nandyal-518501, Andhra Pradesh, India*
[b] *Department of Mathematics, JNTUA College of Engineering, Ananthapuramu-515002, Andhra Pradesh, India*
**Corresponding Author e-mail: dastagiri478@gmail.com*
Received October 7, 2023; revised November 15, 2023; accepted November 17, 2023

Numerical model is conducted to investigate the behavior of an incompressible Maxwell nanofluid model flow on a convectively stretched surface, considering the effects of thermophoresis and an inclined magnetic field. The system, originally formulated as a set of partial differential equations, is transformed into a system of ordinary differential equations using similarity transformations. The resulting equations are solved using the Runge-Kutta-Fehlberg method in conjunction with the shooting technique. The obtained physical parameters from the derived system are presented and discussed through graphical representations. The numerical process is assessed by comparing the results with existing literature under various limiting scenarios, demonstrating a high level of proficiency. The key findings of this study indicate that the velocity field decreases as the fluid parameters increase, while the fluid temperature diminishes accordingly. Additionally, the heat transfer rate decreases with increasing fluid and thermophoresis parameters, but it increases with Biot and Prandtl numbers.
Keywords: *MHD; Nano fluid; Maxwell fluid; Thermophoresis; Activation energy*
PACS: 44.05.+e, 44.40.+a, 47.65.-d, 47.70.Fw

INTRODUCTION

Non-Newtonian fluid flow is fast growing field of interest due to its various applications in different fields of engineering (Rivlin and Ericksen [1]). Examples of these applications include hot rolling paper manufacturing, optical fiber production, plastic polymer processing, cosmetic procedures, and many others. In everyday life, numerous substances such as melts, soaps, apple sauce, soaps, emulsions, shampoos, and blood exhibit the properties of non-Newtonian fluids. Since there is no single constitutive relation that can accurately describe the behavior of such materials, researchers have proposed various models to study the characteristics of non-Newtonian fluids comprehensively. Therefore, different models have been developed in the forms of (i) differential-type, (ii) rate-type, and (iii) integral-type models (Hayat et al. [2]). The rate-type model takes into account the effects of relaxation and retardation times.

Among these models, the Maxwell model belongs to the rate-type category and specifically accounts for the impact of relaxation time, which cannot be captured by differential-type models. The Maxwell fluid model is particularly useful for analyzing polymers with low molecular weight. In a study conducted by Sudarmozhi et al. [3], it was demonstrated that the continuous flow of an MHD Maxwell viscoelastic fluid on a porous plate result in radiation and heat generation. Ibrahim et al. [4] investigated the mixed convection flow of a Maxwell nanofluid with the inclusion of Hall and ion-slip effects, employing the spectral relaxation method. Seshra et al. [5] focused on discussing the convection heat-mass transfer of a generalized Maxwell fluid, taking into account radiation effects, exponential heating, and chemical reactions using fractional Caputo-Fabrizio derivatives. Khan et al. [6] explored the flow of a Maxwell nanofluid over an infinitely tall vertical plate with ramped and isothermal wall temperature and concentration. Shateyi and Hillary [7] conducted a numerical analysis on the unsteady flow of a thermomagnetic reactive Maxwell nanofluid over a stretching or shrinking sheet, considering ohmic dissipation and Brownian motion. In their research, Jawad et al. [8] conducted an analytical study on the mixed convection flow of an MHD Maxwell nanofluid, considering variable thermal conductivity as well as Soret and Dufour effects. Reddy and Reddy [9] performed a comparative analysis of unsteady and steady flows of Buongiorno's Williamson nanoliquid over a wedge, $ShRe_r^{-1/2} = -\phi'(0)$; taking slip effects into account. Jamir and Konwar [10] investigated the effects of radiation absorption, Soret and Dufour effects, as well as slip condition and viscous dissipation on the unsteady MHD mixed convective flow past a vertical permeable plate. In separate studies, various authors [11, 12, 13, 14] explored the behavior of radioactive nanoparticles with exponential heat source and slip effects on an inclined permeable stretching surface. Additionally, authors [15, 16, 17] examined the heat and mass transfer of an MHD nanofluid with chemical reaction on a rotating disk under convective boundary conditions.

Heat transfer plays a crucial role in various industrial and consumer products. However, traditional working liquids like water, ethylene glycol, and oil exhibit low thermal conductivity, posing a significant challenge in improving heat transport within engineering systems. In contrast, metals possess higher thermal conductivities compared to liquids.

Cite as: D.D. Babu, S. Venkateswarlu, E.K. Reddy, East Eur. J. Phys. 4, 326 (2023), https://doi.org/10.26565/2312-4334-2023-4-43

To overcome this limitation, the thermal performance of conventional working liquids has been improved by incorporating ultrafine nanoparticles into the base liquids. The goal of adding nanoparticles to liquids is to enhance the thermal properties of regular fluids. In their research, Huang et al. [18] focused on investigating the influence of the Prandtl number on free convection heat transfer from a vertical plate to a non-Newtonian fluid. Rahbari et al. [19] presented both analytical and numerical solutions for the heat transfer and MHD flow of a non-Newtonian Maxwell fluid through a parallel plate channel. Khan et al. [20] conducted an analysis of the flow of a non-Newtonian fluid past a stretching or shrinking permeable surface, considering heat and mass transfer effects. Liu and Liancun [22] examined the unsteady flow and heat transfer characteristics of a Maxwell nanofluid in a finite thin film, taking into account internal heat generation and thermophoresis. Arulmozhi et al. [22] provided an analysis of heat and mass transfer effects, including radioactive and chemical reactive effects, on MHD nanofluid flow over an infinite moving vertical plate. Vijay et al. [23] conducted a numerical investigation on the dynamics of stagnation point flow of a Maxwell nanofluid, considering combined heat and mass transfer effects.

Activation energy refers to the minimum energy required to initiate a chemical reaction. Once the reaction commences, the activation energy of the system becomes zero. The Arrhenius equation is commonly used to describe this relationship and is expressed as. $K = B\left(T/T_{\infty}\right)^{n} \exp\left(-Ea/\kappa T\right)$. The activation energy for a specific reaction can be determined by analyzing the rate constant's variation with temperature using the Arrhenius equation. The concept of activation energy finds application in various fields, including geothermal engineering, chemical engineering, oil emulsions, and food processing. In their study, Zhang et al. [24] investigated the influence of activation energy and thermal radiation on bio-convection flow of rate-type nanoparticles around a stretching or shrinking disk. Bhatt et al. [25] examined the impact of activation energy on the movement of gyrotactic microorganisms in a magnetized nanofluid flowing past a porous plate. Gangadhar et al. [26] considered the effects of nonlinear radiation, viscous dissipation, and activation energy on a convective heat transfer in a Maxwell fluid. Dessie [27] explored the effects of chemical reaction, activation energy, and thermal energy on the flow of a magnetohydrodynamics (MHD) Maxwell fluid in a rotating frame. Saini et al. [28] studied the combined effects of activation energy and convective heat transfer on the radiative Williamson nanofluid flow over a radially stretching surface, taking into account Joule heating and viscous dissipation. Vaddemani et al. [29] investigated the effects of Hall current, activation energy, and diffusion thermo on the flow of an MHD Darcy-Forchheimer Casson nanofluid in the presence of Brownian motion and thermophoresis.

Upon reviewing the existing research, it is evident that no prior studies have explored the axi-symmetric flow of Maxwell fluid, combined with nanoparticles, over a radially stretched surface. Therefore, the main objective of this study is to investigate the impact of an aligned magnetic field and activation energy on Maxwell nanofluid. Additionally, the study will consider the passive control of nanoparticles at the surface. By conducting this analysis, a deeper understanding of the combined effects and potential control mechanisms can be obtained.

MATHEMATICAL FORMULATION

The flow being considered is a steady axi-symmetric two-dimensional (r, z) flow of a Maxwell liquid with nano-particles induced by a sheet that is stretched radially. The flow occurs in the region where z is greater than or equal to 0, with a sheet velocity $u = u_w = ar$ in the radial direction and w in the z-direction. The parameter 'a' is a positive number. An aligned magnetic field with strength of B_0 is applied along the z-direction at an acute angle γ, as depicted in Figure 1. The effects of activation energy and chemical reaction are accounted for in mass transfer, while the convective temperature is denoted by T_f and the heat transport coefficient is h_f. Additionally, a zero-mass flux condition is enforced at the surface. Under these assumptions, the governing equations for the flow of Maxwell nanofluid are as follows:

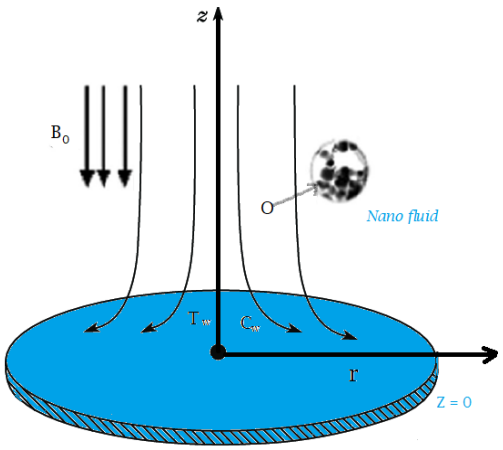

Figure 1. Schematic diagram of the problem

$$\frac{\partial u}{\partial r}+\frac{\partial w}{\partial z}+\frac{u}{r}=0 \tag{1}$$

$$u\frac{\partial u}{\partial r}+w\frac{\partial u}{\partial z}=\upsilon\frac{\partial^2 u}{\partial z^2}-k_0\left(u^2\frac{\partial^2 u}{\partial r^2}+2uw\frac{\partial^2 u}{\partial r\partial z}+w^2\frac{\partial^2 u}{\partial z^2}\right)-\frac{\sigma B_0(r)}{\rho_f}usin^2\gamma \tag{2}$$

$$u\frac{\partial T}{\partial r}+w\frac{\partial T}{\partial z}=\frac{k}{\rho c_p}\frac{\partial^2 T}{\partial z^2}+\tau D_B\frac{\partial T}{\partial z}\frac{\partial C}{\partial z}+\tau\frac{D_T}{T_\infty}\left[\frac{\partial T}{\partial z}\right]^2 \tag{3}$$

$$u\frac{\partial C}{\partial r}+w\frac{\partial C}{\partial z}=D_B\frac{\partial^2 C}{\partial z^2}+\frac{D_T}{T_\infty}\frac{\partial^2 T}{\partial z^2}-k_r{}^2\{C-C_\infty\}\left(\frac{T}{T_\infty}\right)^n e\wedge\left(\frac{-E_a}{kT}\right) \tag{4}$$

With boundary conditions

$$\left.\begin{array}{l} u=u_w+\mathrm{L}\dfrac{\partial u}{\partial z};\ w=0;\ D_B\dfrac{\partial C}{\partial z}+\left(\dfrac{D_B}{T_\infty}\right)\dfrac{\partial T}{\partial z}=0;\ (-k)\dfrac{\partial T}{\partial z}=h_f\left(T_f-T\right)\ at\ z=0 \\ u=0;\ T=T_\infty;\ \ C=C_\infty\ \ as\ \ \ z\to\infty \end{array}\right\} \tag{5}$$

In the given context, (u,w) represents the velocity components in the radial (r) and axial (z) directions, respectively. σ signifies the electrical conductivity, α denotes the thermal diffusivity, k_0 represents the relaxation time of the fluid, υ signifies the kinematic viscosity, ρ denotes the density of the base fluid, D_T signifies the thermophoresis diffusion coefficient, D_B refers to the Brownian diffusion coefficient, and $\tau=\dfrac{(\rho c)_p}{(\rho c)_f}$ represents the ratio of nanoparticle heat capacity to the base fluid heat capacity.

To facilitate the analysis, we introduce the following similarity transformations:

$$\theta=\frac{T-T_\infty}{T_f-T_\infty};\ \ \eta=\sqrt{\frac{a}{\upsilon}}z;\ \phi=\frac{C-C_\infty}{C_f-C_\infty};\ \ u=arf'(\eta);\ \ \mathrm{w}=-2\sqrt{a\upsilon}f(\eta); \tag{6}$$

Through the utilization of Equation (6), the fulfillment of the equation of continuity requirement is achieved automatically. Furthermore, Equations (2)–(5) undergo a transformation into a system of ordinary differential equations (ODEs), accompanied by the imposition of suitable boundary conditions.

$$\frac{d^3 f}{d\eta^3}-\left(\frac{df}{d\eta}\right)^2+2f\left(\frac{d^2 f}{d\eta^2}\right)+\beta\left(4f\left(\frac{df}{d\eta}\right)\left(\frac{d^2 f}{d\eta^2}\right)-4f^2\frac{d^3 f}{d\eta^3}\right)-M\left(\frac{df}{d\eta}\right)sin^2\gamma=0 \tag{7}$$

$$\frac{d^2\theta}{d\eta^2}+2Prf\frac{d\theta}{d\eta}+PrNb\frac{d\theta}{d\eta}\frac{d\phi}{d\eta}+PrNt\left(\frac{d\theta}{d\eta}\right)^2=0 \tag{8}$$

$$\frac{d^2\phi}{d\eta^2}+2Scf\frac{d\phi}{d\eta}+\left(\frac{Nt}{Nb}\right)\frac{d^2\theta}{d\eta^2}-Sc\sigma\left(1+\delta\theta\right)^n e\wedge\left(\frac{-E}{1+\delta\theta}\right)\phi=0 \tag{9}$$

The corresponding boundary conditions are

$$\left.\begin{array}{l} f(0)=0;\ \ f'(0)=1+sf'';\ \ \theta(0)=1+\dfrac{\theta'(0)}{Bi};\ \ Nt\theta'+Nb\phi'=0\ \ at\ \ \eta=0 \\ f'\to 0;\ \ \theta\to 0;\ \ \phi\to 0\ \ \ \ \ as\ \ \eta\to\infty \end{array}\right\} \tag{10}$$

In Equations (6)–(9), the key parameters are defined as follows:

$M=\dfrac{\sigma B_0{}^2}{\rho_a}$, $\beta=ak_0$, $\mathrm{Pr}=\dfrac{\upsilon}{\alpha}$, $Sc=\dfrac{\upsilon}{D_B}$, $Nt=\dfrac{\tau D_T}{\upsilon}\left(\dfrac{T_f-T_\infty}{T_\infty}\right)$, $Nb=\dfrac{\tau D_T}{\upsilon}(C_\infty)$, $Bi=\sqrt{\dfrac{\upsilon}{a}}\left(\dfrac{h_f}{k}\right)$, $\sigma=\dfrac{k_r{}^2}{\alpha}$, $\delta=\dfrac{\left(T_f-T_\infty\right)}{T_\infty}$.

To quantify the skin friction coefficient, local Nusselt number, and Sherwood number, providing valuable insights into the flow characteristics, heat transfer, and mass transfer properties of the system, we can follow

$$C_f Re_r^{1/2} = (1+\beta) f''(0); \quad Nu Re_r^{-1/2} = -\theta'(0);$$

Here $Re_r = \dfrac{U_w(r) r}{\upsilon}$ is the local Reynolds number.

METHODOLOGY

The initial step in the shooting scheme (Ali et al. [30]) involves obtaining numerical solutions by fixing the value of η_∞. The shooting method aims to transform boundary conditions (BCs) into initial conditions (ICs) in order to obtain numerical solutions for the desired system. A detailed procedure outlining the entire process can be found in Table 1, while Fig. 2 provides a visual representation of the method.

Table 1. Mathematical steps for shooting technique

$f = g_1, f' = g_2, f'' = g_3, \ \theta = g_4, \ \theta' = g_5, \phi = g_6, \phi' = g_7$
$g_1' = g_2, g_2' = g_3, \ g_4' = g_5, \ g_6' = g_7$
g_3'
g_5'
g_7'

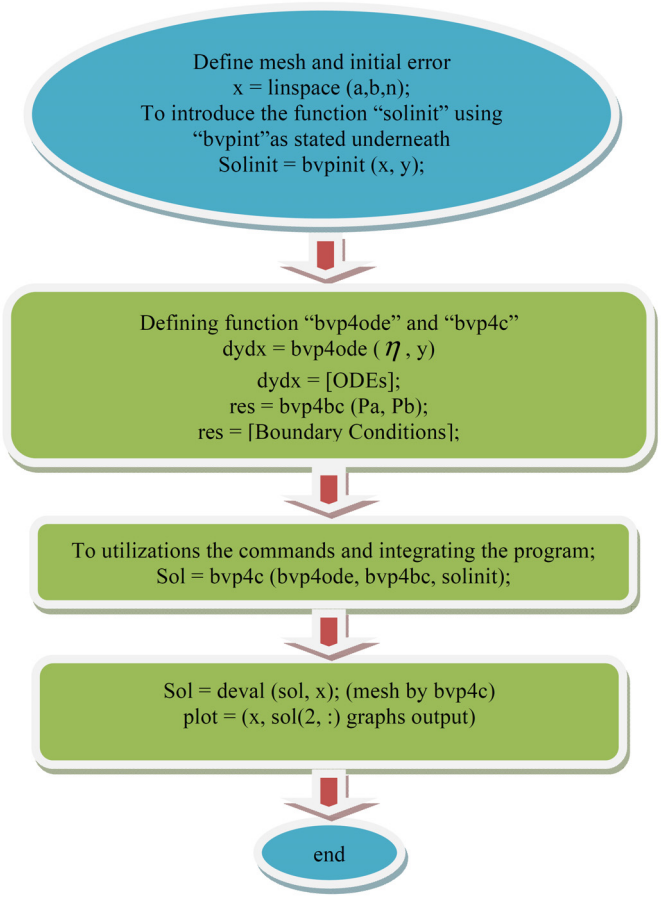

Figure 2. Solution chart via Matlab Procedure

For getting a clear view of the corporal problem, numerical calculations have been continued by the method explained in the preceding section for variety values of dissimilar parameters. For illustrations of the outcomes, numerical data are plotted in figures 3-19. To validate the present solution, comparison has been made with Xu and Eric [31] published data from the literature to $-f''(0)$ for various values of M when $\beta = 0$ in Table 2, and they are found to be in a favorable agreement.

Figures 3–5 depict the impact of parameter M on velocity, temperature, and concentration field. In Figure 3, as M enlarges, a noticeable decrease in velocity can be observed. This behavior is attributed to the rise in Lorentz force, a resistive force that opposes fluid flow. Consequently, the fluid velocity decreases, and the momentum layer becomes thinner. Figure 4 reveals that rising M leads to higher liquid temperatures, as the resistive force grows stronger. The effect of M on the concentration profile is shown in Figure 5, where it is evident that increasing M results in an incremental change in the profile.

Figures 6–8 illustrate the influence of the elasticity parameter β on velocity, temperature, and concentration field. These graphs reveal that an increase in β leads to a decrease in velocity and the associated momentum layer, while the opposite trend is observed for temperature and concentration distribution.

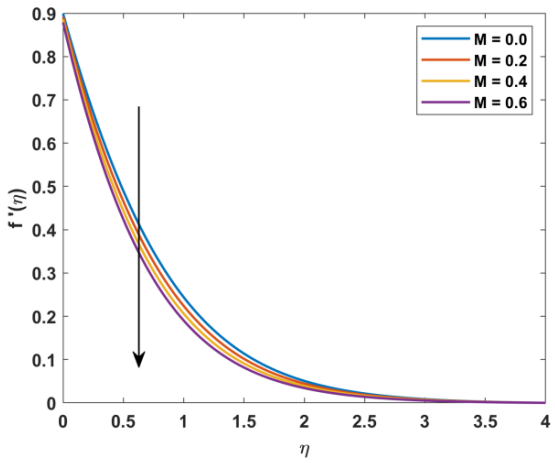

Figure 3. Impact $f'(\eta)$ on M

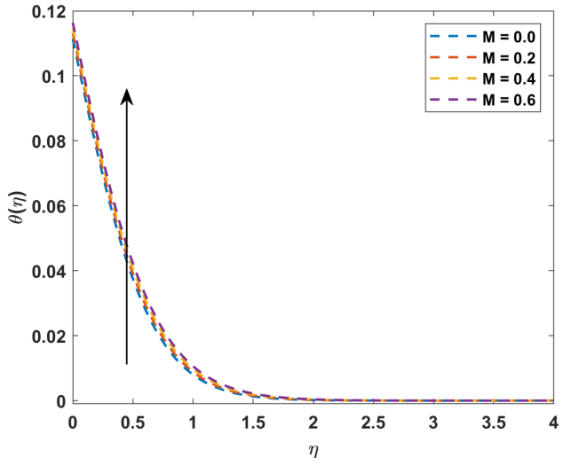

Figure 4. Impact $\theta(\eta)$ on M

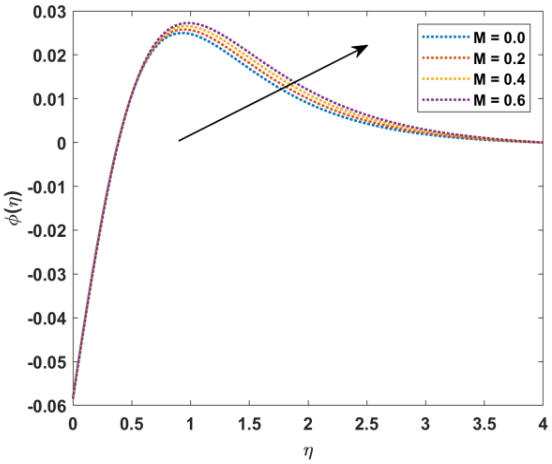

Figure 5. Impact $\phi(\eta)$ on M

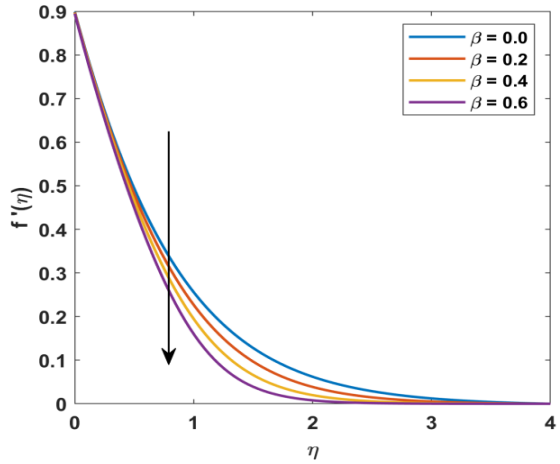

Figure 6. Impact $f'(\eta)$ on Beta

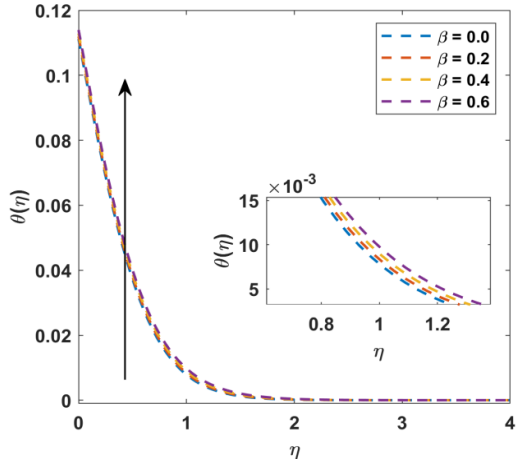

Figure 7. Impact $\theta(\eta)$ on Beta

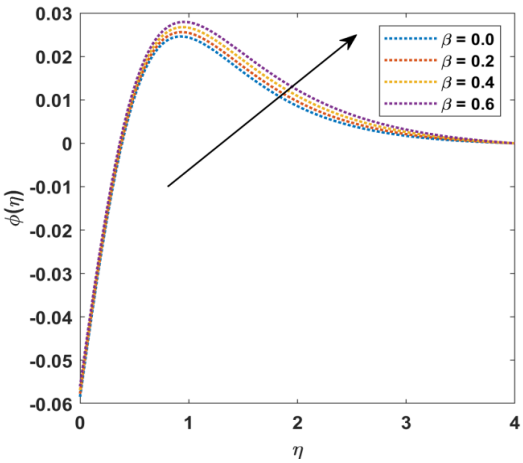

Figure 8. Impact $\phi(\eta)$ on Beta

The elasticity parameter β is related to the relaxation time, which represents the time required for the liquid to reach equilibrium after the application of stress. Smaller values of β result in liquid-like behavior, while larger values enhance liquid viscosity, causing a decline in velocity which is noticed in Figure 6. Moreover, for higher β values, the material exhibits solid-like characteristics. In Figure 7, it is evident that an increase in β leads to higher temperatures and a thicker corresponding layer over time. This behavior can be attributed to the influence of relaxation time, which becomes larger as β increases. Figure 8 clearly demonstrates that the concentration field increases as the magnetic number β rises.

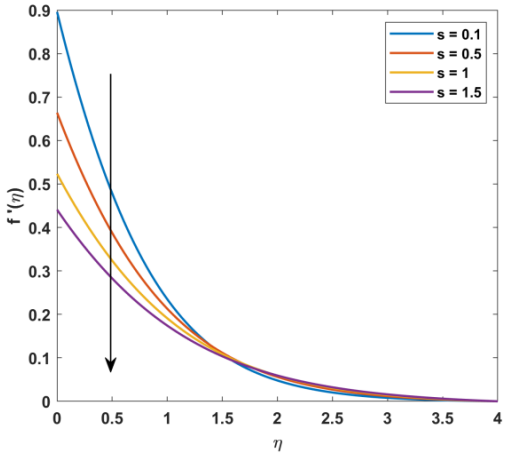

Figure 9. Impact $f'(\eta)$ on S

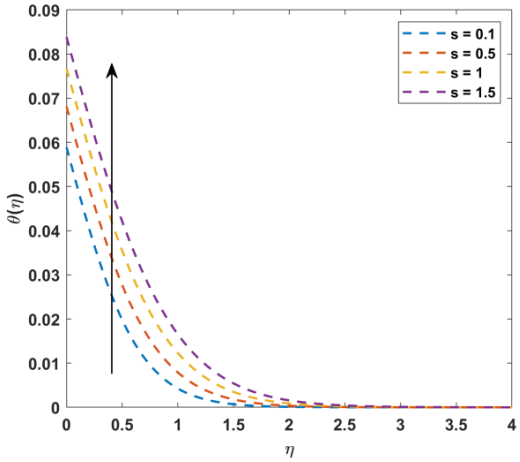

Figure 10. Impact $\theta(\eta)$ on S

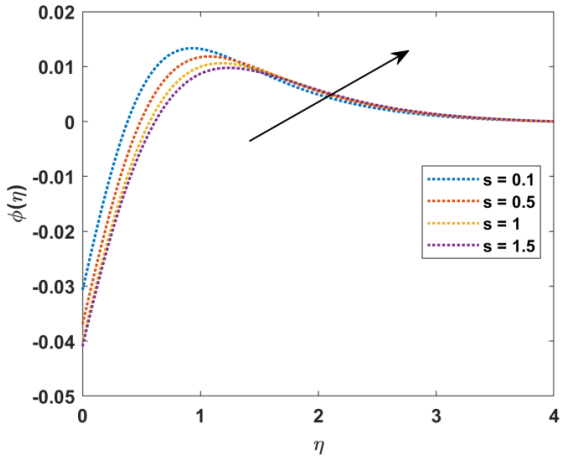

Figure 11. Impact $\phi(\eta)$ on S

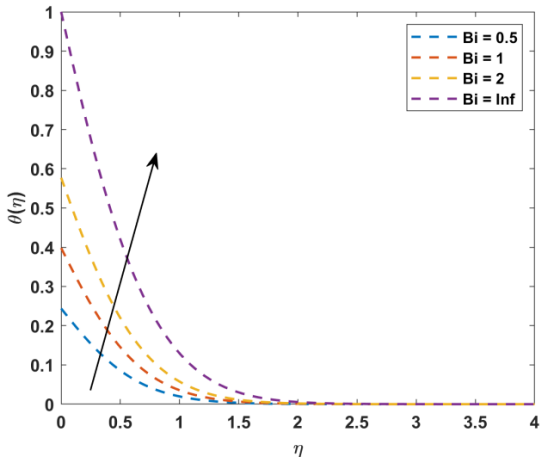

Figure 12. Impact $\theta(\eta)$ on Bi

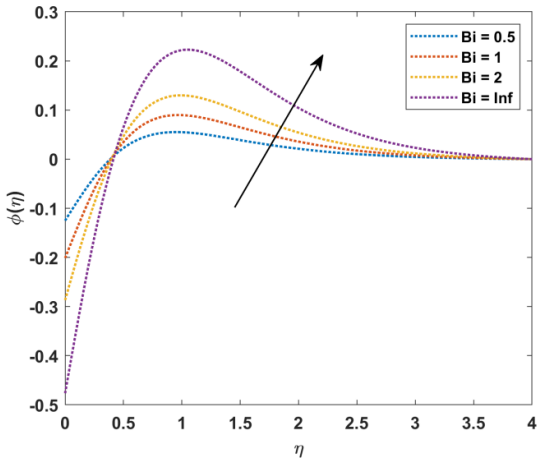

Figure 13. Impact $\phi(\eta)$ on Bi

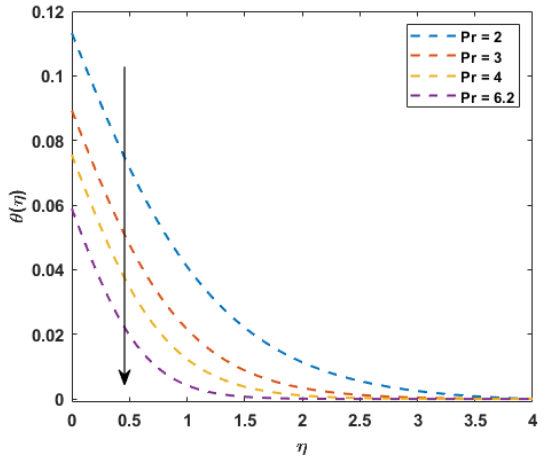

Figure 14. Impact $\theta(\eta)$ on Pr

Figures 9-11 demonstrate the influence of the velocity slip parameter (s) on the distributions of velocity, temperature, and concentration. An observed trend is a decline in the velocity profile as the s values increase. This is

because higher s values result in stretching effects partially penetrating the fluid, causing a decrease in velocity, and it is depicted in figure (9). Moreover, from figure (10), and figure (11), an increase in s values is observed to enhance both temperature and concentration profiles. When s = 0, the fluid adheres to the boundary and slides with no resistance $s \to \infty$. However, as s values increase, the movement of fluid particles decreases, leading to an increase in both temperature and concentration.

Figure 12 and 13 depicts the impact of the Biot number (Bi) on temperature (θ) and concentration (ϕ) profiles. It is evident from the figure that an increase in Bi leads to an enlargement of $\theta(\eta)$ as well as $\phi(\eta)$. Furthermore, it can be observed that an enhancement in the Biot number results in an increase in the heat transfer coefficient, which in turn contributes to an increment in $\theta(\eta)$.

Figures 14 and 15 are presented to analyze the influence of the Prandtl number (Pr) on $\theta(\eta)$, and $\phi(\eta)$, representing temperature and thermal layer thickness, respectively. In physical terms, Pr is inversely proportional to thermal conductivity. As a result, an increase in Pr leads to a weaker thermal diffusion. Consequently, both the temperature $\theta(\eta)$ and concentration $\phi(\eta)$ profiles decrease.

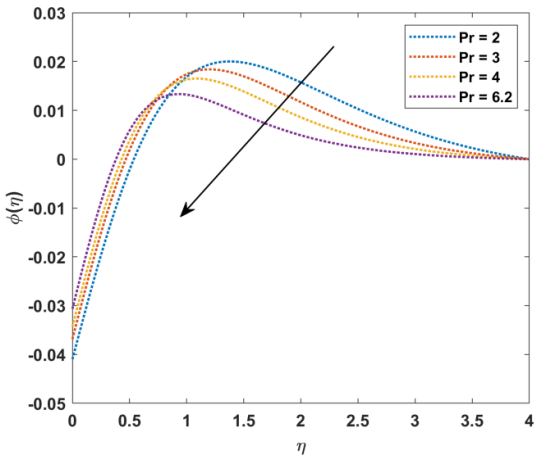

Figure 15. Impact $\phi(\eta)$ on Pr

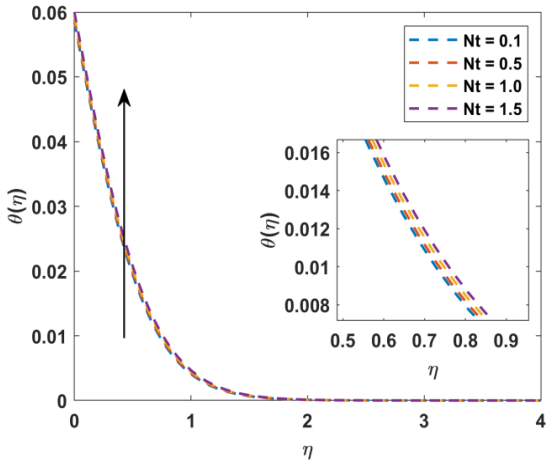

Figure 16. Impact $\theta(\eta)$ on Nt

Figures 16 and 17 illustrate the impact of thermophoresis (Nt) on nanofluid temperature and concentration fields. Both distributions show a similar trend, with an increase in Nt. However, in Figure 18, the opposite trend is observed for the augmentation of Nb the concentration distribution. Physically, as Nt increases, more nanoparticles are transported from the hotter surface to the colder region. This results in an increase in the temperature and concentration of the nanofluid. On the other hand, due to the random nature of Brownian motion, the concentration exhibits a decreasing tendency against Nb.

Figure 19 is plotted to observe the variation of $\phi(\eta)$ with respect to the activation energy (E). It can be observed that both $\phi(\eta)$ and its layer thickness increase as E values increase. Additionally, it was noticed that higher activation energy and less temperature decay result in a decrease in the reaction rate, leading to a decline in the chemical reaction mechanisms. As a result, the concentration of the Maxwell nanofluid increases.

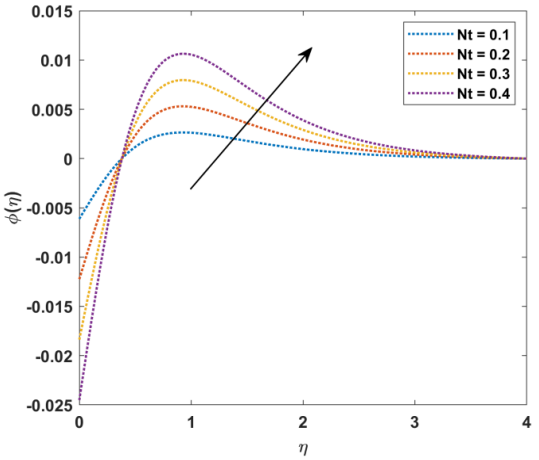

Figure 17. Impact $\phi(\eta)$ on Nt

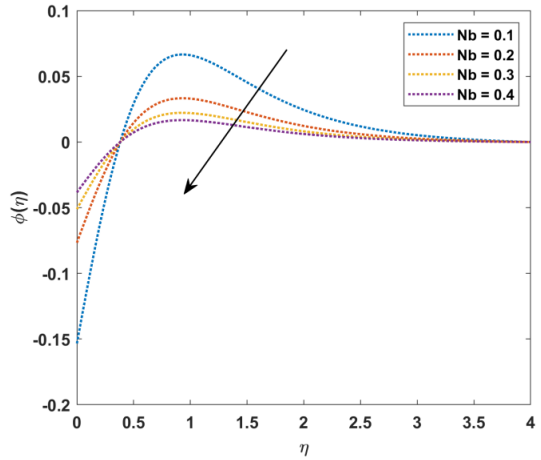

Figure 18. Impact $\theta(\eta)$ on Nb

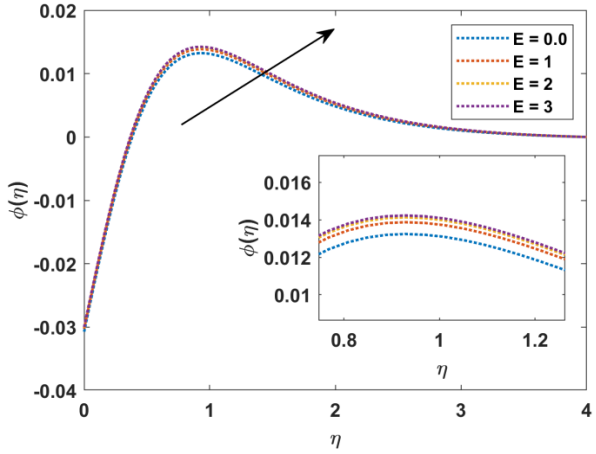

Figure 19. Impact on E

Table 2. Comparison of $-f''(0)$ for various values of M when $\beta = 0$.

M	Xu and Eric [31]	Present Results
1	1.41421	1.414032
5	2.4494	2.449456
10	3.3166	3.316624
50	7.1414	7.141424
100	10.0498	10.049896
500	22.38302	22.383032

CONCLUSION

The Maxwell's nanofluid model of incompressible, hydromagnetic flow is reduced using the Runge-Kutta-Fehlberg method with the shooting technique. This reduction is accomplished through the use of similarity variables. Additionally, the effects of inclined magnetic strength and thermophoresis are taken into account. The numerical analysis yields the following findings regarding the physical parameters:

- The momentum boundary layer decreases as the parameter β increases.
- An increase in the parameter M results in a decrease in the flow field f'(η), while an increase in the parameter γ elevates it.
- The parameters Sc and σ contribute to the reduction of the concentration curves, while an increase in the parameter M enhances the concentration field.
- The thermal field θ(η) and its associated boundary layer decrease with proper increments in the parameters Pr and γ. However, the opposite effect is observed when the parameters Bi and Nt are enhanced.
- The Sherwood number accelerates as the parameter β increases.
- The Nusselt number increases with the parameters Bi and Pr.

ORCID

D. Dastagiri Babu, https://orcid.org/0000-0001-8114-3860; **S. Venkateswarlu,** https://orcid.org/0009-0004-8224-374X
E. Keshava Reddy, https://orcid.org/0000-0003-3880-0989

REFERENCES

[1] R.S. Rivlin, and J.L. Ericksen, "*S*tress-deformation relations for isotropic materials," J. Rational Mech. Anal. **4**, 323–425 (1955). https://doi.org/10.1512/iumj.1955.4.54011
[2] T. Hayat, M. Mustafa, S. A. Shehzadand, and S. Obaidat, "Meltingheat transfer in the stagnation-point flow of an upper-convected Maxwell (UCM) fluid past a stretching sheet," Int. J. Numer. Meth. Fl., **68**, 233–243 (2012). https://doi.org/10.1002/fld.2503
[3] K. Sudarmozhi, D. Iranian, and Ilyas Khan, "A steady flow of MHD Maxwell viscoelastic fluid on a flat porous plate with the outcome of radiation and heat generation," Frontiers in Physics, **11**, (2023). https://doi.org/10.3389/fphy.2023.1126662
[4] W. Ibrahim and T. Anbessa, "Mixed convection flow of a Maxwell nanofluid with Hall and ion-slip impacts employing the spectral relaxation method," Heat Transfer, **49**(5), 3094-3118 (2020). https://doi.org/10.1002/htj.21764
[5] Sehra, H. Sadia, N. Gul, A. Zeb, and Z. A. Khan, "Convection heat–mass transfer of generalized Maxwell fluid with radiation effect, exponential heating, and chemical reaction using fractional Caputo–Fabrizio derivatives," Open Physics, **20**(1), 1250-1266 (2022). https://doi.org/10.1515/phys-2022-0215
[6] N. Khan, F. Ali, M. Arif, Z. Ahmad, A. Aamina, and I. Khan, "Maxwell nanofluid flow over an infinite vertical plate with ramped and isothermal wall temperature and concentration," Mathematical Problems in Engineering, **2021**, 1-19 (2021). https://doi.org/10.1155/2021/3536773

[7] S. Shateyi, and H. Muzara, "A numerical analysis on the unsteady flow of a thermomagnetic reactive Maxwell nanofluid over a stretching/shrinking sheet with ohmic dissipation and Brownian motion," Fluids, **7**(8), 252 (2022). https://doi.org/10.3390/fluids7080252
[8] M. Jawad, A. Saeed, A. Khan, I. Ali, H. Alrabaiah, T. Gul, E. Bonyah, and M. Zubair, "Analytical study of MHD mixed convection flow for Maxwell nanofluid with variable thermal conductivity and Soret and Dufour effects," AIP Advances, **11**(3), (2021). https://doi.org/10.1063/5.0029105
[9] R. Chandra Sekhar Reddy, and P. Sudarsana Reddy, "A comparative analysis of unsteady and steady Buongiorno's Williamson nanoliquid flow over a wedge with slip effects," Chinese Journal of Chemical Engineering, **28**(7), 1767-1777 (2020). https://doi.org/10.1016/j.cjche.2020.04.016
[10] T. Jamir, and H. Konwar, "Effects of Radiation Absorption, Soret and Dufour on Unsteady MHD Mixed Convective Flow past a Vertical Permeable Plate with Slip Condition and Viscous Dissipation," Journal of Heat and Mass Transfer Research, **9**(2), 155-168 (2022). https://doi.org/10.22075/jhmtr.2023.28693.1399
[11] T. Abbas, K. Al-Khaled, A.H. Raza, M. Ayadi, W. Chammam, and S.U. Khan, "Inclined Magnetized Flow of Radioactive Nanoparticles with Exponential Heat Source and Slip Effects: Keller Box Simulations," Journal of Nanofluids, **12**(2), 571-579 (2023). https://doi.org/10.1166/jon.2023.1935
[12] S. Shah, S. M. Atif, and A. Kamran, "Radiation and slip effects on MHD Maxwell nanofluid flow over an inclined surface with chemical reaction," Heat Transfer, **50**(4), 4062-4085 (2021). https://doi.org/10.1002/htj.22064
[13] A.B. Patil, V.S. Patil, P.P. Humane, N.S. Patil, and G.R. Rajput, "Thermally and chemically reacted MHD Maxwell nanofluid flow past an inclined permeable stretching surface," Proceedings of the Institution of Mechanical Engineers, Part E: Journal of Process Mechanical Engineering, **236**(3), 838-848 (2022). https://doi.org/10.1177/09544089211050715
[14] B.K. Taid, and N. Ahmed, "MHD free convection flow across an inclined porous plate in the presence of heat source, Soret effect, and chemical reaction affected by viscous dissipation Ohmic heating," Biointerface Research in Applied Chemistry, **12**(5), 6280-6296 (2022). https://doi.org/10.33263/BRIAC125.6280-6296
[15] S.M. Upadhya, R.L.V. Renuka Devi, C.S.K. Raju, and H.M. Ali, "Magnetohydrodynamic nonlinear thermal convection nanofluid flow over a radiated porous rotating disk with internal heating," Journal of Thermal Analysis and Calorimetry, **143**, 1973-1984 (2021). https://doi.org/10.1007/s10973-020-09669-w
[16] M.S. Arif, Y. Nawaz, M. Bibi, and Z. Ali, "Mass Transfer of MHD Nanofluid in Presence of Chemical Reaction on A Permeable Rotating Disk with Convective Boundaries, Using Buongiorno's Model," CMES-Computer Modeling in Engineering & Sciences, **116**(1), (2018). https://doi.org/10.31614/cmes.2018.03834
[17] I. Ali, T. Gul, and A. Khan, "Unsteady Hydromagnetic Flow over an Inclined Rotating Disk through Neural Networking Approach. Mathematics," **11**(8), 1893 (2023). https://doi.org/10.3390/math11081893
[18] M. Huang, J. Huang, Y. Chou, and C.O. Chen, "Effects of Prandtl number on free convection heat transfer from a vertical plate to a non-Newtonian fluid. Journal of Heat Transfer," Transcations of the ASME Series C, **111**(1), (1989). https://doi.org/10.1115/1.3250645
[19] A. Rahbari, M. Abbasi, I. Rahimipetroudi, B. Sundén, D. DomiriGanji, and M. Gholami, "Heat transfer and MHD flow of non-Newtonian Maxwell fluid through a parallel plate channel: analytical and numerical solution," Mechanical Sciences, **9**(1), 61-70 (2018). https://doi.org/10.5194/ms-9-61-2018
[20] S. Khan, M.M. Selim, A. Khan, A. Ullah, T. Abdeljawad, Ikramullah, M. Ayaz, and W. K. Mashwani, "On the analysis of the non-Newtonian fluid flow past a stretching/shrinking permeable surface with heat and mass transfer," Coatings, **11**(5), 566 (2021). https://doi.org/10.3390/coatings11050566
[21] T. Liu, L. Lin, and L. Zheng, "Unsteady flow and heat transfer of Maxwell nanofluid in a finite thin film with internal heat generation and thermophoresis," Thermal Science, **22**(6 Part B), 2803-2813 (2018). https://doi.org/10.2298/TSCI170129097L
[22] S. Arulmozhi, K. Sukkiramathi, S. S. Santra, R. Edwan, U. Fernandez-Gamiz, and S. Noeiaghdam, "Heat and mass transfer analysis of radiative and chemical reactive effects on MHD nanofluid over an infinite moving vertical plate," Results in Engineering **14**, 100394 (2022). https://doi.org/10.1016/j.rineng.2022.100394
[23] N. Vijay, and K. Sharma, "Dynamics of stagnation point flow of Maxwell nanofluid with combined heat and mass transfer effects: A numerical investigation," International Communications in Heat and Mass Transfer **141**, 106545 (2023). https://doi.org/10.1016/j.icheatmasstransfer.2022.106545
[24] T. Zhang, S. U. Khan, M. Imaran, I. Tlili, H. Waqas, N. Ali, "Activation energy and thermal radiation aspects in bioconvection flow of rate-type nanoparticles configured by a stretching/shrinking disk," Journal of Energy Resources Technology, **142(**11), 112102 (2020). https://doi.org/10.1115/1.4047249
[25] M.M. Bhatti, A. Shahid, T. Abbas, S.Z. Alamri, and R. Ellahi, "Study of activation energy on the movement of gyrotactic microorganism in a magnetized nanofluids past a porous plate," Processes, **8(**3), 328, (2020). https://doi.org/10.3390/pr8030328
[26] K. Gangadhar, D. Vijayakumar, and K. Thangavelu, "Nonlinear radiation on Maxwell fluid in a convective heat transfer with viscous dissipation and activation energy," Heat Transfer, **50(**7), 7363-7379 (2021). https://doi.org/10.1002/htj.22233
[27] H. Dessie, "Effects of Chemical Reaction, Activation Energy and Thermal Energy on Magnetohydrodynamics Maxwell Fluid Flow in Rotating Frame," Journal of Nanofluids, **10**(1), 67-74 (2021). https://doi.org/10.1166/jon.2021.1767
[28] S. K. Saini, R. Agrawal, and P. Kaswan, "Activation energy and convective heat transfer effects on the radiative Williamson nanofluid flow over a radially stretching surface containing Joule heating and viscous dissipation," Numerical Heat Transfer, Part A: Applications, 1-24 (2023). https://doi.org/10.1080/10407782.2023.2226815
[29] V. Ramachandra Reddy, G. Sreedhar, and K. Raghunath, "Effects of Hall Current, Activation Energy and Diffusion Thermo of MHD Darcy-Forchheimer Casson Nanofluid Flow in the Presence of Brownian Motion and Thermophoresis," Journal of Advanced Research in Fluid Mechanics and Thermal Sciences, **105(**2), 129-145, (2023). https://doi.org/10.37934/arfmts.105.2.129145
[30] M. Ali, M. Shahzad, F. Sultan, W.A. Khan, and S.Z.H. Shah, "Characteristic of heat transfer in flow of Cross nanofluid during melting process," Applied Nanoscience, **10**, 5201-5210, (2020). https://doi.org/10.1007/s13204-020-01532-6
[31] L. Xu, and E.W.M. Lee, "Variational iteration method for the magnetohydrodynamic flow over a nonlinear stretching sheet," Abstract and Applied Analysis, Hindawi, **2013**, 1085-3375 (2013). https://doi.org/10.1155/2013/573782

ЧИСЕЛЬНЕ ДОСЛІДЖЕННЯ ЕФЕКТІВ ТЕРМОФОРЕЗУ ТА ЕНЕРГІЇ АКТИВАЦІЇ НАНОРІДИНИ МАКСВЕЛЛА НАД НАХИЛЕНИМ МАГНІТНИМ ПОЛЕМ, ПРИКЛАДЕНИМ ДО ДИСКА

Д. Дастагірі Бабу[a], С. Венкатесварлу[a], Е. Кешава Редді[b]

[a] Кафедра математики, меморіальний коледж інженерії та технології Раджива Ганді, Нандьял-518501, Андхра-Прадеш, Індія

[b] Факультет математики, інженерний коледж JNTUA, Анантхапураму-515002, Андхра-Прадеш, Індія

Розроблена числова модель для дослідження поведінки течії моделі нестисливої нанорідини Максвелла на конвективно розтягнутій поверхні з урахуванням ефектів термофорезу та похилого магнітного поля. Система, спочатку сформульована як набір рівнянь у частинних похідних, перетворюється на систему звичайних диференціальних рівнянь за допомогою перетворень подібності. Отримані рівняння розв'язуються за допомогою методу Рунге-Кутта-Фельберга в поєднанні з технікою стрільби. Отримані фізичні параметри похідної системи представлені та обговорені за допомогою графічних зображень. Чисельний процес оцінюється шляхом порівняння результатів з існуючою літературою за різними сценаріями обмеження, що демонструє високий рівень кваліфікації. Основні висновки цього дослідження вказують на те, що поле швидкості зменшується зі збільшенням параметрів рідини, тоді як температура рідини відповідно зменшується. Крім того, швидкість тепловіддачі зменшується зі збільшенням параметрів рідини та термофорезу, але зростає із збільшенням чисел Біо та Прандтля.

Ключові слова: *МГД; нанорідина; рідина Максвелла; термофорез; енергія активації*